Journal of Electroanalytical Chemistry 967 (2024) 118482

Contents lists available at ScienceDirect

Journal of Electroanalytical Chemistry

journal homepage: www.elsevier.com/locate/jelechem

Layer-by-layer assembled film of TiO_2/poly(L-lysine)/graphene quantum dots for simultaneous electrochemical determination of guanine and adenine

Raril Chenthattil [a], Sijian Luo [a,b], Hang Ao [a], Wencheng Xiao [a], Huangxian Ju [a,*]

[a] State Key Laboratory of Analytical Chemistry for Life Science, School of Chemistry and Chemical Engineering, Nanjing University, Nanjing 210023, PR China
[b] Department of Laboratory Medicine, The Affiliated Hospital of Southwest Medical University, Luzhou 646000, PR China

ARTICLE INFO

Keywords:
Electrochemical biosensor
Electropolymerization
Graphene quantum dots
TiO_2 nanoparticles
L-lysine
Square wave voltammetry
Adenine
Guanine

ABSTRACT

This work proposed an electrochemical biosensing method for simultaneous detection of guanine and adenine. This electrochemical biosensor was constructed by layer-by-layer assembling TiO_2 nanoparticles, poly(L-lysine) and graphene quantum dots (GQDs) on a glassy carbon electrode. The assembled film of TiO_2/poly(L-lysine)/GQDs showed better conductivity and significantly increased effective surface area for the electrochemical oxidation of guanine and adenine along with a quasi-reversible electrode process. Under optimal preparation and square wave voltammetric detection conditions, the proposed electrochemical methods could simultaneously detect guanine and adenine ranging from 1.0 to 35.0 μM with detection limits of 0.56 μM for GA and 0.81 μM for AD. The limits of quantification for sample analysis were 1.90 and 2.70 μM, respectively. The developed electrochemical biosensor exhibited good reproducibility, anti-interfering properties, and stability, and could be practically applied in the simultaneous determination of guanine and adenine in calf thymus DNA, cow milk, and urine samples with acceptable precision.

1. Introduction

Guanine (GA) and adenine (AD) are significant purine components that make up the fundamental building blocks of the DNA structure, together with cytosine and thymine, play important roles in life processes [1]. The regulation of blood flow, prevention of cardiac arrhythmias, inhibition of neurotransmitter release, etc are all significantly impacted by GA and AD [2]. Therefore, the detection of these compounds has become very important in clinical fields because the unusual changes of DNA bases in organisms may lead to a deficiency of mutation in the immune system and cause a variety of diseases, including cancer, epilepsy, mental retardation, etc [3]. There have been significant efforts to use modern electrochemical techniques in nucleic acid research and DNA analysis ever since the electroactivity of DNA was discovered. Since GA is the nitrogenous base that oxidizes the easiest, a thorough investigation of its oxidation mechanism has been studied in detail. Several techniques, including chromatography, spectroscopy, capillary electrophoresis, etc, have been developed for the determination of GA and AD [4–6]. All these techniques are very useful, show high sensitivity but time-consuming, and require expensive instruments, pre-treatments, and expert handling. The development of electrochemical nucleic acid biosensors based on the detection of GA and AD oxidation would benefit from this knowledge. Electrochemical methods are attractive due to their low cost, fast detection, simplicity, rapidity, and high sensitivity [7–12]. However, the development of sensitive electrochemical sensors for fast and low-cost detection of GA and AD is still challenging.

Many carbon-based materials such as pyrolytic graphite, glassy carbon and carbon nanotubes have been used as electrode materials for the preparation of electrochemical sensors. However, the direct determination of purine in biological matrices at bare carbon-based electrodes faced many problems, such as high overpotential and poor reproducibility. To solve these issues, ionic liquids [13,14], gold nanoparticles [15], Nafion-ruthenium oxide pyrochlore [16], boron-doped carbon nanotubes [17], magnetic nanoparticles [18], graphene [19,20] and carbon nanotubes [21–24] have been used to modify the electrodes for improving the performance of GA and AD sensing. TiO_2 nanoparticles (rutile) have also been incorporated on carbon or carbon-based materials modified electrode surface to improve the electrochemical sensing performance of GA and AD due to their unique

* Corresponding author.
E-mail address: hxju@nju.edu.cn (H. Ju).

https://doi.org/10.1016/j.jelechem.2024.118482
Received 10 April 2024; Received in revised form 11 June 2024; Accepted 30 June 2024
Available online 2 July 2024

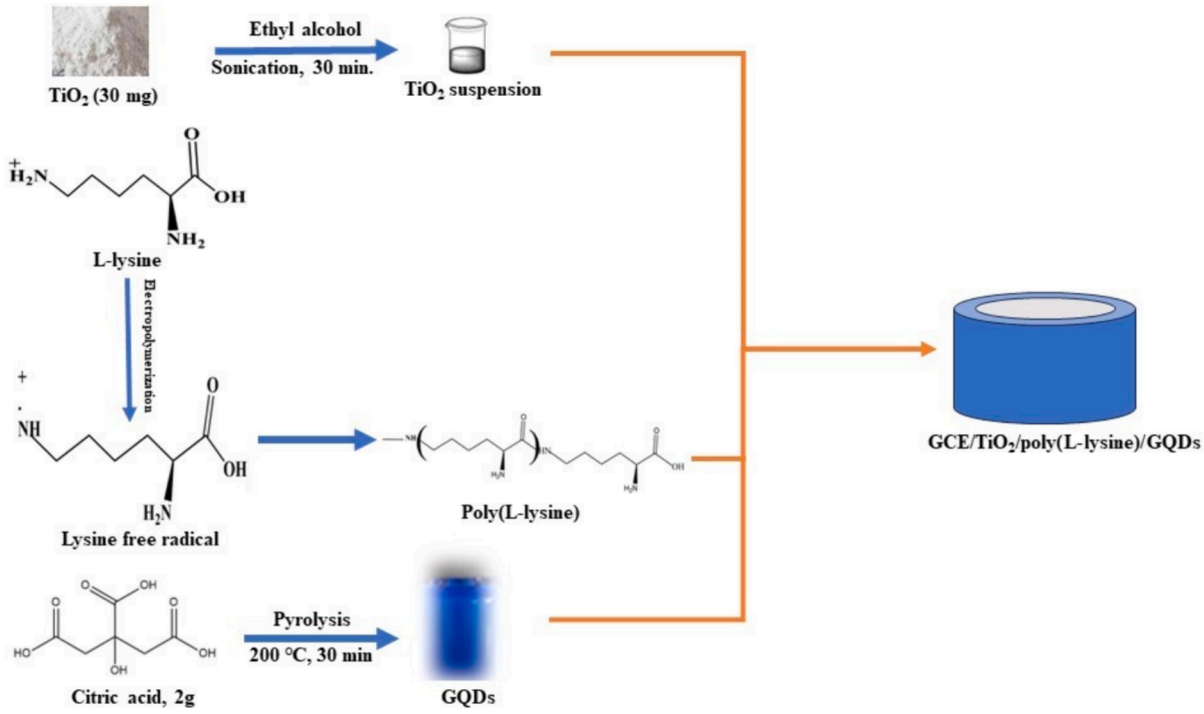

Scheme 1. Synthetic processes of TiO_2/poly(L-lysine)/GQDs composite material.

properties such as biocompatibility, absorptivity, and catalytic properties [25–28].

To improve the physical and chemical properties of modified electrode, the electrode modification with different polymers has also attracted much attention for sensor preparation. These polymers can be conveniently prepared in situ by electropolymerization technique, and show the advantages of uniform deposition, charge transfer characteristics, good stability, and reproducibility [29–37]. As a conductive polymer, poly(L-lysine) shows many advantages, such as simple preparation, stability, more active sites and availability, and has been widely used in the manufacturing of some sensors for trace metals [38], proteins [39], cancer cells [40], and glucose [41]. Therefore, this work integrated the advantages of poly(L-lysine) and TiO_2 nanoparticles with the high conductivity and catalytic properties of graphene quantum dots (GQDs), a type of zero-dimensional nanosized fragments of graphene [42–46], to construct a sensitive electrochemical biosensor for the simultaneous determination of GA and AD.

The assembled film of TiO_2/poly(L-lysine)/GQDs possessed high conductivity and significantly increased effective surface area for the oxidation of guanine and adenine, leading to excellent analytical performance of the proposed electrochemical detection method, such as appropriate range of detectable concentration, low detection limit, and good reproducibility, anti-interfering properties and stability. The proposed method could successfully be applied for the quantification of GA and AD in calf thymus DNA, cow milk, and urine samples, demonstrating a promising modification material for the preparation of electrochemical biosensors.

2. Experimental section

2.1. Chemicals

L-lysine and calf thymus DNA were obtained from Sigma-Aldrich. Monosodium di-hydrogen phosphate (NaH_2PO_4), and disodium hydrogen phosphate (Na_2HPO_4) were obtained from Aladdin. Phosphate buffer solution (PBS) with a concentration of 0.1 M was used as a supporting electrolyte, which was prepared by mixing a suitable quantity of NaH_2PO_4 and Na_2HPO_4. GA and AD were procured from Heowns and stock solutions were prepared by dissolving appropriate amounts of analytes in diluted NaOH (0.2 M) solution. Citric acid and TiO_2 nanoparticles (rutile, 60 nm) were purchased from Macklin. NaOH, KCl, HCl, and $K_3[Fe(CN)_6]$ were purchased from Nanjing Chemical Reagent Co. Ltd. All reagents were used as received without further purification. Ultrapure water (≥18.2 MΩ, Milli-Q, Millipore) was used throughout the experiment.

2.2. Apparatus

A CHI 630D potentiostat was used to conduct all the electrochemical measurements with Pt wire as counter, saturated calomel electrode (SCE) as reference electrode, and glassy carbon electrode (GCE) or modified GCE as working electrodes. The solution pH was monitored using a pH meter from BANTE Instrument. Field emission scanning electron microscopic (FE-SEM) measurements were carried out using a JSM-7800F instrument, operating at 5.0 kV. Transmission electron microscopy (TEM) was performed using a JEM-2800 instrument, operating at 100 kV.

2.3. Preparation of graphene quantum dots and samples

GQDs were synthesized through the pyrolysis of citric acid at an elevated temperature. In brief, 2 g citric acid was heated at a temperature of 200 ℃ for 30 min, which showed the color change from colorless to pale yellow, and ultimately produce an orange liquid, indicating the formation of GQDs. Subsequently, 100 mL of 10 mg mL^{-1} NaOH was added while stirring continuously, and the pH was adjusted to 8.0 with 1 mol/L HCl to ensure the stability of GQDs [47,48].

3 mg of calf thymus DNA was digested with 1 mL of 1 M HCl over a boiling water bath for 1 h. Afterward, the solution pH was adjusted to neutral with 1 M NaOH. Cow milk samples was bought from the nearest local supermarket, and the urine samples (1 mL of each sample was dissolved in 25 mL of PBS, and the experiment was carried out with the standard addition method) were collected from the healthy volunteer, which were detected by adding the sample in 0.1 M pH 7.0 PBS without

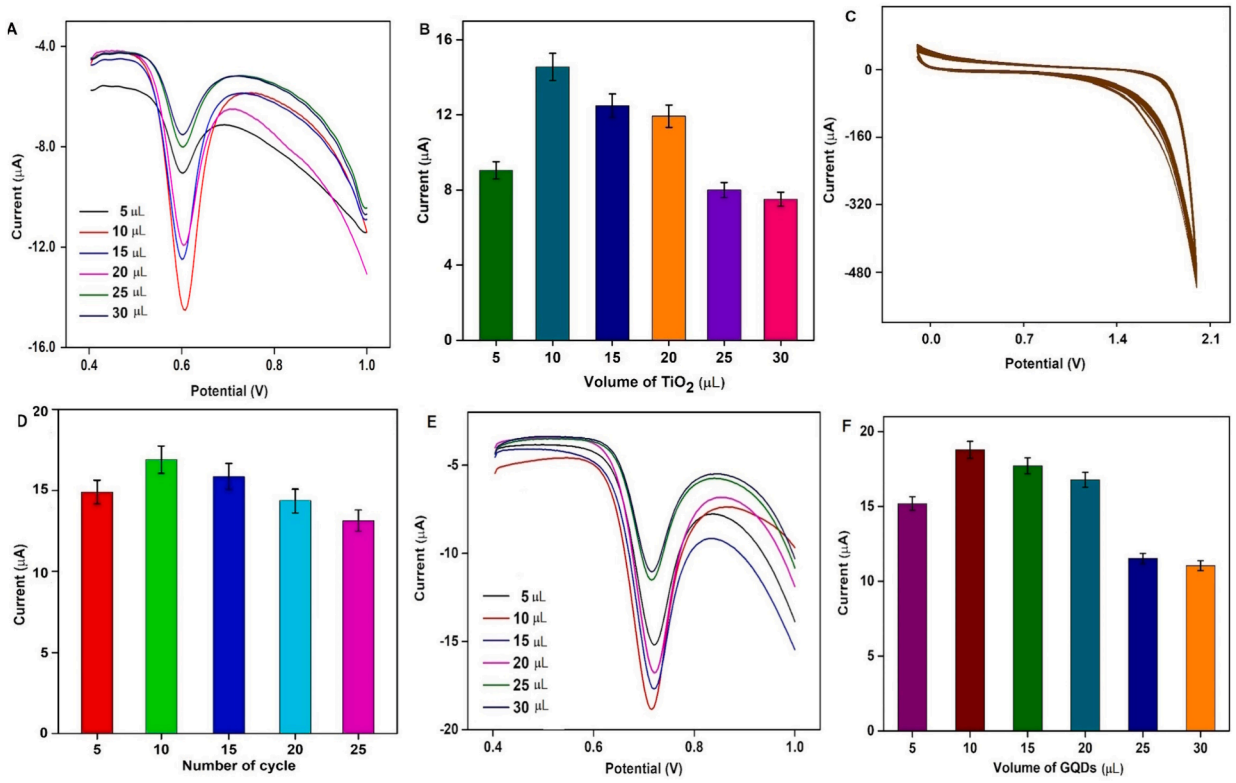

Fig. 1. (**A**) Square wave voltammograms of 10 μM GA at GCE/TiO_2/poly(L-lysine)/GQDs prepared with different volumes of TiO_2 suspension (3 mg/mL). **(B)** Peak currents of 10 μM GA at different volumes of TiO_2 suspension. (**C**) Continuously cyclic voltammogram for electropolymerization of 1 mM L-lysine at GCE/TiO_2 in 0.1 M pH 5.0 PBS at 0.1 V/s. (**D**) Peak currents of 10 μM GA at different cycle numbers for polymerization. (**E**) Square wave voltammograms of 10 μM GA at different volumes of GQDs (1 mg/mL) coated at GCE/TiO_2/poly(L-lysine). (**F**) Peak currents of 10 μM GA at different volumes of GQDs.

any pretreatment.

2.4. Biosensor preparation

GCE (2 mm in diameter) was polished to a reflective finish using a polishing pad with 0.3 and 0.05 μm alumina slurry. The electrode was then sonicated with ethyl alcohol and ultrapure water to remove any residual polishing materials. GCE/TiO_2 was obtained by casting an appropriate amount of TiO_2 suspension, which was prepared by adding 30 mg TiO_2 nanoparticles in 10 mL ethyl alcohol to sonicate for 30 min, on the freshly prepared GCE to dry for 5 min. Poly(L-lysine) was then electropolymerized on GCE/TiO_2 in 0.1 M PBS (pH 5.0) containing 1.0 mM L-lysine by sweeping the potential between −0.1 and + 2.0 V at 0.1 V/s for 10 cycles. After rinsing the electrode with ultrapure water, 10 μL GQDs (1 mg/mL) was coated on its surface to obtain GCE/TiO_2/poly(L-lysine)/GQDs as the biosensor for simultaneous detection of GA and AD. Scheme 1 illustrates the synthetic processes of TiO_2/poly(L-lysine)/GQDs composite material.

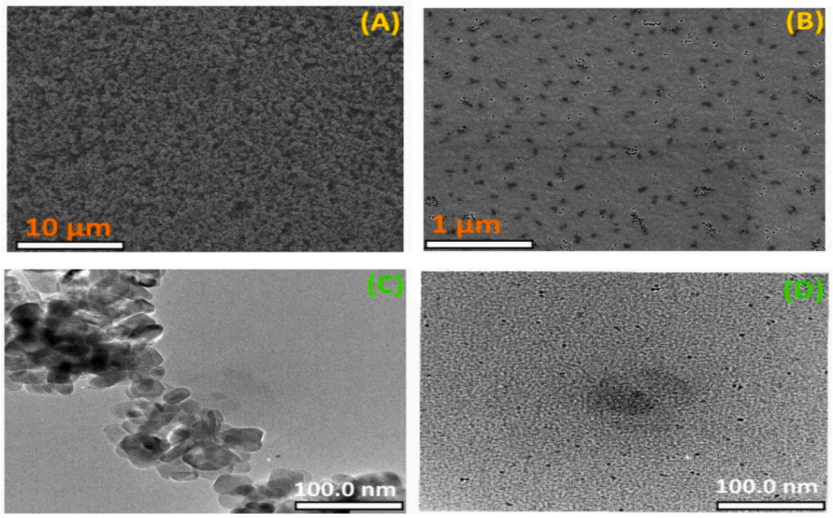

Fig. 2. (**A, B**) FE-SEM and (**C, D**) TEM images of TiO_2 nanoparticles (**A, C**) and GQDs (**B, D**).

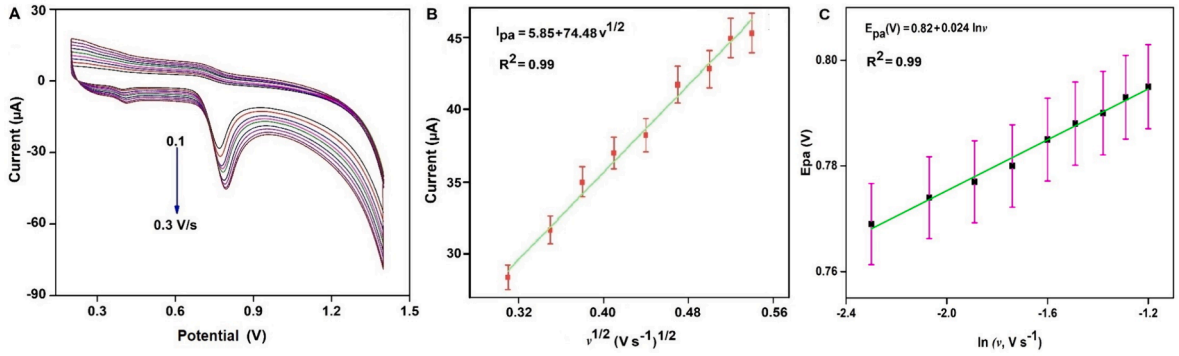

Fig. 3. (**A**) Cyclic voltammograms of 100 μM GA at GCE/TiO_2/poly(L-lysine)/GQDs at 0.1 to 0.3 V/s in 0.1 M pH 7.0 PBS, (**B**) Plot of I_{pa} vs $v^{1/2}$, (**C**) Plot of E_{pa} vs ln v.

3. Results and discussion

3.1. Optimization of preparation conditions

The volume of TiO_2 suspension for the preparation of the biosensor was optimized by measuring the square wave voltammetric (SWV) response of 10 μM GA in 0.1 pH 7.0 PBS at GCE/TiO_2/poly(L-lysine)/GQDs. As shown in Fig. 1A, B, with the increasing volume of TiO_2 suspension (3 mg/mL), the current response of GA increased, and reached the maximum value at 10 μL, which was thus used as an optimal volume. The increased response resulted from the unique properties of TiO_2 such as biocompatibility and catalytic properties [25–28]. The response decrease at a higher volume of TiO_2 suspension could be attributed to the increased electron transfer impedance because the assembled film became too thick.

The continuously cyclic voltammogram of 1 mM L-lysine at GCE/TiO_2 in 0.1 M pH 5.0 PBS was shown in Fig. 1C, which indicated obvious electropolymerization of L-lysine on the electrode surface, and led to increasing SWV response of 10 μM GA at GCE/TiO_2/poly(L-lysine)/GQDs (Fig. 1D) due to the presence of positively charged poly(L-lysine) to interact with negatively charged GA. The possible electropolymerization mechanism of L-lysine on the surface could be described as follows: the monomer L-lysine was oxidized at high potentials to produce the free radical form of amino, which bound with the surface group on GCE/TiO_2 [49]. After 10 cycles of polymerization, the SWV response gradually decreased due to the increase of polymer film thickness, which restricted electron exchange between GA and electrode.

The amount of GQDs on GCE/TiO_2/poly(L-lysine)/GQDs greatly affected the electrochemical response of 10 μM GA at the electrode (Fig. 1E). With the increasing amount of GQDs, the peak current of square wave voltammogram increased quickly (Fig. 1F), which was attributed to the high conductivity of GQDs to improve the electron transfer of electrode surface for the oxidation of GA. After the volume of 10 μL, the peak current gradually decreased. As a result, 10 μL of 1 mg/mL GQDs was used for the preparation of the biosensor.

3.2. Characterization of nanoparticles

The FE-SEM image of TiO_2 nanoparticles showed their agglomeration in nature [49] (Fig. 2A), while the FE-SEM image of GQDs showed small particles dispersed uniformly without any agglomeration (Fig. 2B), which led to a large surface area upon the casting of GQDs on electrode surface. The TEM image demonstrated a cube-like structure of TiO_2 nanoparticles with a size of about 60 nm (Fig. 2C). The TEM image of GQDs revealed the dark spherical particles with 4–6 nm in size (Fig. 2D), as observed in [48].

3.3. Electroactive surface areas and electrochemical responses of GA at different electrodes

The cyclic voltammograms of 2.0 mM $K_3[Fe(CN)_6]$ at different GCEs were shown in Fig. S1. With the successive layer-by-layer assembly of TiO_2 nanoparticles, poly(L-lysine), and GQDs, the peak current of $[Fe(CN)_6]^{3-}$ increased, and the difference of cathodic and anodic peak potentials slightly decreased, indicating the increased electron transfer rate and active surface area. The increased charging current upon assembly of GQDs on GCE/TiO_2/poly(L-lysine) (Fig. S1) demonstrated the increase in active surface area. From the Randles-Sevcik equation [50]: $I_p = 2.65 \times 10^5 n^{3/2} A D^{1/2} v^{1/2} c$, where I_p represents the peak current, n

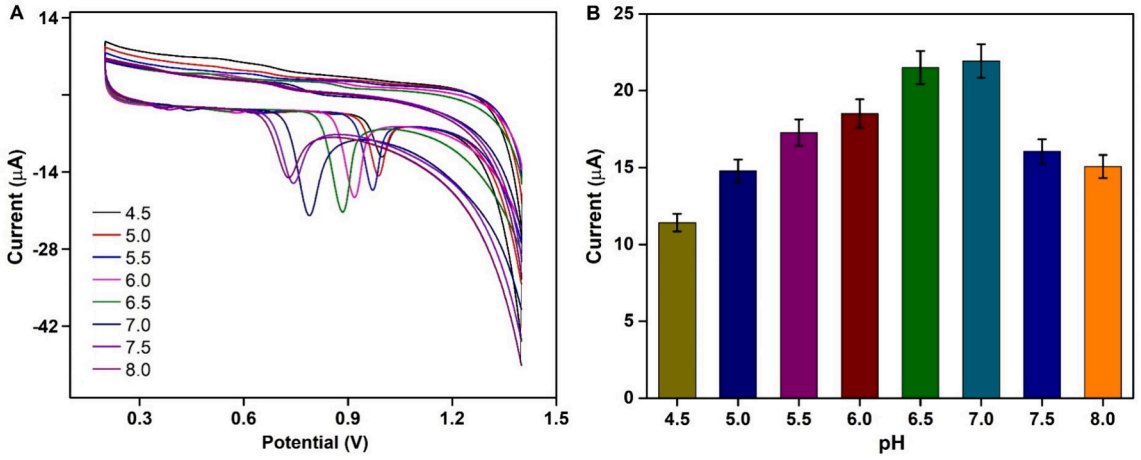

Fig. 4. (**A**) Cyclic voltammograms of 100 μM GA in 0.1 M PBS (pH 4.5–8.0) at GCE/TiO_2/poly(L-lysine)/GQDs at 0.1 V/s. (**B**) I_{pa} at different pHs.

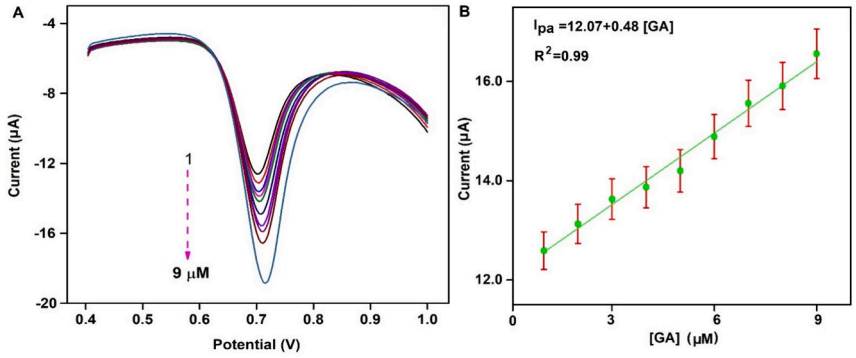

Fig. 5. (**A**) Square wave voltammograms of GA at 1.0 to 9.0 μM at GCE/TiO_2/poly(L-lysine)/GQDs in 0.1 M pH 7.0 PBS. (**B**) Plot of I_{pa} vs concentration of GA.

denotes the number of electrons involved in the electrode reaction, A refers to the effective surface area (cm^2), *c* represents the concentration of electroactive species (mol/mL), D is the diffusion coefficient (7.6×10^{-6} cm^2s^{-1}), and *v* is the scan rate (V/s), the surface areas of GCE, GCE/TiO_2, GCE/TiO_2/poly(L-lysine) and GCE/TiO_2/poly(L-lysine)/GQDs were calculated to be 0.05, 0.06, 0.07 and 0.15 cm^2, respectively. Thus, the GCE/TiO_2/poly(L-lysine)/GQDs showed the quick electron transfer and the maximum active surface area for the oxidation of analytes on the electrode surface.

The electrochemical responses of analytes at GCE, GCE/TiO_2, GCE/TiO_2/poly(L-lysine), and GCE/TiO_2/poly(L-lysine)/GQD were examined with square wave voltammetry (SWV). At bare GCE, both GA and AD showed weak oxidation peaks, which increased with the successive assembly of TiO_2 nanoparticles, poly(L-lysine) and GQDs along with negative shift of the oxidation peak potentials (Fig. S2 and S3), indicating the accelerated electron transfer due to the improved conductivity and the increased active surface area.

With the increasing scan rate from 0.1 to 0.3 V/s, the oxidation peak current of GA at GCE/TiO_2/poly(L-lysine)/GQDs increased, and the peak potential positively shifted (Fig. 3A). The plot of peak current vs $v^{1/2}$ showed a linear relationship (Fig. 3B), while the oxidation peak potential was proportional to the logarithm of scan rate, indicating a quasi-reversible electrode process. From the slope of the plot of peak potential vs ln*v* (Fig. 3C), the αn value (α is charge transfer coefficient, n is the electron transfer number was calculated to be 2.13 [51].

3.4. Effect of solution pH on GA response

The oxidation of GA at GCE/TiO_2/poly(Lysine)/GQDs showed obvious dependence on solution pH (Fig. 4A). With the increasing pH, the oxidation peak potential moved in the negative direction, indicating that the oxidation of GA was a deprotonation process. While the oxidation peak current of GA increased until pH 7.0, exhibiting easier-to-follow redox activities with higher peak currents and catalytic activity, and then decreased with further increase in pH (Fig. 4B), which indicated an optimum solution pH for the electrochemical detection of GA.

3.5. SWV detection of guanine

With the increasing concentration of GA at pH 7.0, the SWV response at GCE/TiO_2/poly(Lysine)/GQDs increased (Fig. 5A), and the plot of peak current vs GA concentration in the range of 1.0–9.0 μM showed good linearity (Fig. 5B). The linear regression equation was $I_{pa}(A) = 12.07 + 0.48\ [GA]_{\mu M}$ ($R^2 = 0.99$), from which the limit of detection was calculated to be 0.44 μM at three times the standard deviation (5 measurements of the blank), and the limit of quantification was calculated as ten times the standard deviation (5 measurements of the blank) to be 1.48 μM [52].

3.6. Simultaneous SWV determination of guanine and adenine

In the presence of 1.0 μM AD, the square wave voltammograms of GA with increasing concentration (Fig. S4A) showed the increasing peak current at the same potential at GCE/TiO_2/poly(L-lysine)/GQDs, as those in the absence of AD (Fig. 5A), and the plot of peak current vs GA concentration also showed good linearity (Fig. S4B). Meanwhile, the peak current of AD linearly increased with the increasing AD concentration in the presence of 1.0 GA (Fig. S4C, D). Therefore, the coexistence of AD and GA did not affect their electrochemical oxidation, and GCE/TiO_2/poly(L-lysine)/GQDs could well distinguish their responses, leading to an electrochemical method for simultaneous SWV determination of guanine and adenine.

The SWV responses of both GA and AD increased with the simultaneously increasing concentrations (Fig. S4E). The plots of peak currents vs GA and AD concentrations resulted in the linear regression equations of $I_{pa}(\mu A) = 13.80 + 0.32\ [GA]_{\mu M}$ ($R^2 = 0.98$) and $I_{pa}(\mu A) = 19.21 + 0.46\ [AD]_{\mu M}$ ($R^2 = 0.99$), respectively (Fig. S4F). The limits of qualification were 1.90 μM for GA, and 2.70 μM for AD, and the detection limits were 0.56 and 0.81 μM for GA and AD, respectively, which were comparable with those reported previously (Table S1).

3.7. Interference, reproducibility and stability

The anti-interference properties of the developed biosensor was examined by detecting the SWV signals of 10 μM GA in the presence of different metal ions, such as Ca^{2+}, Cl^-, Cu^{2+}, Fe^{3+}, K^+, Zn^{2+} and some other compounds such as glucose, L-cystein, glycine and urea. The signal changes of GA were found to be < 2 % at 50-fold concentration of Ca^{2+}, Cl^-, Cu^{2+}, Fe^{3+}, K^+, Zn^{2+} and some other compounds such as glucose, L-cystein, glycine and urea, indicating the good selectivity of the designed sensor.

The reproducibility of the biosensor was evaluated by measuring the electrochemical responses of GA using 4 independently prepared biosensors. The relative standard deviation was 4 %, which demonstrated the satisfactory reproducibility of the developed biosensor. In addition, the stability of the developed biosensor was also tested by consecutive potential scanning for 100 cycles, which did not show any change in peak potential, and the peak current could retain 86.6 % of the initial value, indicating acceptable stability.

3.8. Sample testing

The developed biosensor was used for the simultaneous determination of GA and AD in calf thymus DNA, cow milk, and urine samples. After these samples were treated, respectively, two SWV peaks corresponding to GA and AD oxidation could be readily detected. In calf thymus DNA, GA and AD were found in the molar ratio of 22.9 % and 30.8 %, respectively. The ratio of (G + C)/(A + T) was found to be 0.74, which was close to the standard value of 0.77 [53]. The detection results

Table 1
Detection of GA and AD in urine and milk samples.

Sample	Added (μM)		Found (μM)	Recovery (%)	
	GA	AD	GA	AD	
Urine	1.0	1.06	1.00	106.0	100.7
	2.0	2.00	1.91	100.4	95.9
	3.0	2.97	2.91	99.3	97.0
Cow milk	1.0	1.00	0.90	100.4	90.4
	2.0	1.90	1.86	95.0	93.0
	3.0	2.90	2.94	96.8	98.0

of cow milk and urine samples were listed in Table 1. The recovery rates of GA and AD ranged between 99.3 to 106.0 %, 95.9 to 100.7 %, and 95.0 to 100.4 %, and 90.4 to 98.0 %, respectively, demonstrating the practicality of the proposed biosensor in real sample analysis of GA and AD.

4. Conclusions

A simple, low-cost and sensitive biosensor has been developed for simultaneous electrochemical detection of GA and AD. The biosensor can be conveniently prepared by successively casting TiO_2 nanoparticles, electropolymerizing poly(L-lysine) and coating GQDs on GCE. The GCE/TiO_2/poly(L-lysine)/GQDs possesses good conductivity and significantly increased effective surface area for the oxidation of guanine and adenine. The sensitive SWV responses of GA and AD at the biosensor can be well distinguished, and the proposed method shows excellent performance along with high selectivity, satisfactory reproducibility, and acceptable stability, and good practicality in real sample analysis of GA and AD.

Declaration of competing interest

The authors declare that they have no known competing financial interests or personal relationships that could have appeared to influence the work reported in this paper.

Acknowledgments

This study was supported by the National Natural Science Foundation of China (Nos.21890741, 21827812)

Appendix A. Supplementary data

Supplementary data to this article can be found online at https://doi.org/10.1016/j.jelechem.2024.118482.

References

[1] W. Saenger, Principles of Nucleic Acid Structure, Springer, New York (1984).
[2] S.P. Li, P. Li, T.T.X. Dong, K.W.K. Tsim, Determination of nucleosides in natural cordyceps sinensis and cultured cordyceps mycelia by capillary electrophoresis, Electrophoresis 22 (2001) 144–150, https://doi.org/10.1002/1522-2683(200101)22:1<144::AID-ELPS144>3.0.CO;2-T.
[3] Q. Shen, X.M. Wang, Simultaneous determination of adenine, guanine, and thymine based on β-cyclodextrin/MWNTs modified electrode, J. Electroanal. Chem. 632 (2009) 149–153, https://doi.org/10.1016/j.jelechem.2009.04.009.
[4] S.Z. Rong, L.N. Zou, Y.N. Zhang, G.T. Zhang, X.X. Li, M.J. Li, F.H. Yang, C.M. Li, Y. J. He, H.J. Guan, Y.P. Guo, D. Wang, X.Y. Cui, H.T. Ye, F.H. Liu, H.Z. Pan, Determination of purine contents in different parts of pork and beef by high-performance liquid chromatography, Food Chem. 170 (2015) 303–307, https://doi.org/10.1016/j.foodchem.2014.08.059.
[5] H.M. Shi, Y. Cui, Y.J. Gong, S. Feng, Highly sensitive and selective fluorescent assay for guanine based on the Cu^{2+}/eosin Y system, Spectrochim, Acta, A. 161 (2016) 150–154, https://doi.org/10.1016/j.saa.2016.02.023.
[6] C.F. Yeh, S.J. Jiang, Determination of monophosphate nucleotides by capillary electrophoresis inductively coupled plasma mass spectrometry, Analyst 127 (2002) 1324–1327, https://doi.org/10.1039/B206850H.
[7] B. Habibi, M. Jahanbakhshi, A glassy carbon electrode modified with carboxylated diamond nanoparticles for differential pulse voltammetric simultaneous determination of guanine and adenine, Microchim. Acta 183 (2016) 2317–2325, https://doi.org/10.1007/s00604-016-1868-6.
[8] K. Barman, S.K. Jasimuddin, Electrochemical detection of adenine and guanine using a self-assembled copper(II)-thiophenyl-azo-imidazole complex monolayer modified gold electrode, RSC Adv. 4 (2014) 49819–49826, https://doi.org/10.1039/C4RA08568J.
[9] J. Chang, W. Xiao, P. Liu, X. Liao, Y. Wen, L. Bai, Carboxymethyl cellulose assisted preparation of water-processable halloysite nanotubular composites with carboxyl-functionalized multi-carbon nanotubes for simultaneous voltammetric detection of uric acid, guanine and adenine in biological samples, J. Electroanal. Chem. 780 (2016) 103–113, https://doi.org/10.1016/j.jelechem.2016.09.013.
[10] L. Svorce, K. Klacher, Modification free electrochemical approach for sensitive monitoring of purine DNA bases: Simultaneous determination of guanine and adenine in biological samples using a boron-doped diamond electrode, Sens. Actuators B 194 (2014) 332–342, https://doi.org/10.1016/j.snb.2013.12.104.
[11] H. Sharma, N. Singh, D.O. Jang, A benzimidazole/benzothiazole-based electrochemical chemosensor for nanomolar detection of guanine, RSC Adv. 5 (2015) 6962–6969, https://doi.org/10.1039/C4RA12892C.
[12] Z.H. Chen, L. Zhang, Y. Liu, J.H. Li, Highly sensitive electrogenerated chemiluminescence biosensor for galactosyltransferase activity and inhibition detection using gold nanorod and enzymatic dual signal amplification, J. Electroanal. Chem. 781 (2016) 83–89, https://doi.org/10.1016/j.jelechem.2016.05.034.
[13] T. Liu, X. Zhu, L. Cui, P. Ju, X. Qu, S. Ai, Simultaneous determination of adenine and guanine utilizing PbO_2-carbon nanotubes-ionic liquid composite film modified glassy carbon electrode, J. Electroanal. Chem. 651 (2011) 216–221, https://doi.org/10.1016/j.jelechem.2010.11.026.
[14] W. Sun, Y. Li, Y. Duan, K. Jiao, Direct electrocatalytic oxidation of adenine and guanine on carbon ionic liquid electrode and the simultaneous determination, Biosens. Bioelectron. 24 (2008) 988–993, https://doi.org/10.1016/j.bios.2008.07.068.
[15] H. Liu, G. Wang, D. Chen, W. Zhang, C. Li, B. Fang, Fabrication of polythionine/NPAu/MWNTs modified electrode for simultaneous determination of adenine and guanine in DNA, Sens. Actuators B, Chem. 128 (2008) 414–421, https://doi.org/10.1016/j.snb.2007.06.028.
[16] J.M. Zen, M.R. Chang, G. Ilangovan, Simultaneous determination of guanine and adenine contents in DNA, RNA and synthetic oligonucleotides using a chemically modified electrode, Analyst 124 (1999) 679–684, https://doi.org/10.1039/A900532C.
[17] C. Deng, Y. Xia, C. Xiao, Z. Nie, M. Yang, S. Si, Electrochemical oxidation of purine and pyrimidine bases based on the boron-doped nanotubes modified electrode, Biosens. Bioelectron. 31 (2012) 469–474, https://doi.org/10.1016/j.bios.2011.11.018.
[18] A.A. Ensafi, M. Jafari-Asl, B. Rezaei, A.R. Allafchian, Simultaneous determination of guanine and adenine in DNA based on $NiFe_2O_4$ magnetic nanoparticles decorated MWCNTs as a novel electrochemical sensor using adsorptive stripping voltammetry, Sens. Actuators B, Chem. 177 (2013) 634–642, https://doi.org/10.1016/j.snb.2012.11.028.
[19] A. Kalaivani, S.S. Narayanan, Simultaneous Determination of Adenine and Guanine Using Cadmium Selenide Quantum Dots-Graphene Oxide Nanocomposite Modified Electrode, J. Nanosci. Nanotechnol. 15 (2015) 4697–4705, https://doi.org/10.1166/jnn.2015.9717.
[20] K.J. Huang, D.J. Niu, J.Y. Sun, C.H. Han, Z.W. Wu, Y.L. Li, X.Q. Xiong, Novel electrochemical sensor based on functionalized graphene for simultaneous determination of adenine and guanine in DNA, Colloids Surf. B 82 (2011) 543–549, https://doi.org/10.1016/j.colsurfb.2010.10.014.
[21] A. Abbaspour, A. Ghaffarinejad, Preparation of a sol–gel-derived carbon nanotube ceramic electrode by microwave irradiation and its application for the determination of adenine and guanine, Electrochim. Acta 55 (2010) 1090–1096, https://doi.org/10.1016/j.electacta.2009.09.065.
[22] X. Tu, X. Luo, S. Luo, L. Yan, F. Zhang, Q. Xie, Novel carboxylation treatment and characterization of multiwalled carbon nanotubes for simultaneous sensitive determination of adenine and guanine in DNA, Microchim. Acta 169 (2010) 33–40, https://doi.org/10.1007/s00604-010-0307-3.
[23] K. Wu, J. Fei, W. Bai, S. Hu, Direct electrochemistry of DNA, guanine and adenine at a nanostructured film-modified electrode, Anal. Bioanal. Chem. 376 (2003) 205–209, https://doi.org/10.1007/s00216-003-1887-0.
[24] C. Tang, U. Yogeswaran, S. Chen, Simultaneous determination of adenine guanine and thymine at multi-walled carbon nanotubes incorporated with poly(new fuchsin) composite film, Anal. Chim. Acta 636 (2009) 19–27, https://doi.org/10.1016/j.aca.2009.01.055.
[25] B. Filanovsky, B. Markovsky, T. Bourenko, N. Perkas, R. Persky, A. Gedanken, D. Aurbach, Carbon electrodes modified with TiO_2/metal nanoparticles and their application for the detection of trinitrotoluene, Adv. Funct. Mater. 17 (2007) 1487–1492, https://doi.org/10.1002/adfm.200600714.
[26] D. Spitzer, T. Cottineau, N. Piazzon, S. Josset, F. Schnell, S.N. Pronkin, E. R. Savinova, V. Keller, Bio-inspired nanostructured sensor for the detection of ultralow concentrations of explosives, Angew. Chem. Int. Ed. 51 (2012) 5334–5338, https://doi.org/10.1021/jp405050a.
[27] J. Tao, Q. Cuan, S. Halpegamage, R. Addou, X.Q. Gong, M. Batzill, Combined surface science and DFT study of the adsorption of dinitrotoluene (2,4-DNT) on rutile TiO_2 (110): molecular-scale insight into sensing of explosives, J. Phys. Chem. C 117 (2013) 16468–16476, https://doi.org/10.1021/jp405050a.
[28] A.Z. Asl, A.A. Rafati, S. Khazalpour, Electrocatalytic behavior of TiO_2/MWCNTs nanocomposite decorated on glassy carbon electrode for individual and simultaneous voltammetric determination of adenine and guanine in real samples,

J. Electrochem. Soc. 169 (2022) 047516, https://doi.org/10.1149/1945-7111/ac644d.
[29] S.C. Monterroso, H.M. Carapuca, A.C. Duarte, Mixed polyelectrolyte coatings on glassy carbon electrodes: ion-exchange, permselectivity properties and analytical application of poly-l-lysine-poly(sodium 4-styrenesulfonate)-coated mercury film electrodes for the detection of trace metals, Talanta 68 (2006) 1655–16662, https://doi.org/10.1016/j.talanta.2005.08.029.
[30] H. Chen, Y. Cui, B. Zhang, B. Liu, G. Chen, D. Tang, Poly(o-phenylenediamine)-carried nanogold particles as signal tags for sensitive electrochemical immunoassay of prolactin, Anal. Chim. Acta 728 (2012) 18–25, https://doi.org/10.1016/j.aca.2012.03.052.
[31] D. Zhang, Y. Zhang, L. Zheng, Y. Zhan, L. He, Graphene oxide/poly-L-lysine assembled layer for adhesion and electrochemical impedance detection of leukemia K562 cancer cells, Biosens. Bioelectron. 42 (2013) 112–118, https://doi.org/10.1016/j.bios.2012.10.057.
[32] L. Hua, X. Wu, R. Wang, Glucose sensor based on an electrochemical reduced graphene oxide-poly(L-lysine) composite film modified GC electrode, Analyst 137 (2012) 5716–5719, https://doi.org/10.1039/C2AN35612K.
[33] C. Raril, J.G. Manjunatha, Carbon-nanotube-paste-electrode-for-the-determination-of-some-neurotransmitters, Modern Chemistry and applications, Mod. Chem. Appl. 6 (2018) 1000263, https://doi.org/10.4172/2329-6798.1000263.
[34] T.Y. Lee, Y.B. Shim, Direct DNA hybridization detection based on the oligonucleotide-functionalized conductive polymer, Anal. Chem. 73 (2001) 5629–5632, https://doi.org/10.1021/ac015572w.
[35] M.H. Naveen, N.G. Gurudatt, Y.B. Shim, Applications of conducting polymer composites to electrochemical sensors: a review, Appl. Mater. Today 9 (2017) 419–433, https://doi.org/10.1016/j.apmt.2017.09.001.
[36] N.G. Gurudatt, M.H. Naveen, C. Ban, Y.B. Shim, Enhanced electrochemical sensing of leukemia cells using drug/lipid co-immobilized on the conducting polymer layer, Biosens. Bioelectron. 86 (2016) 33–40, https://doi.org/10.1016/J.BIOS.2016.06.029.
[37] Y. Li, H. Wang, B. Yan, H. Zhang, An electrochemical sensor for the determination of bisphenol A using glassy carbon electrode modified with reduced graphene oxide-silver/poly-L-lysine nanocomposites, J. Electroanal. Chem. 805 (2017) 39–46, https://doi.org/10.1016/j.jelechem.2017.10.022.
[38] S. Chen, J. Liu, R. Thangamuthu, Electropreparation of poly(benzophenone-4) film modified electrode and its electrocatalytic behavior towards dopamine, ascorbic acid and nitrite, Electroanalysis 18 (2006) 2361–2368, https://doi.org/10.1002/elan.200603672.
[39] C. Raril, J.G. Manjunatha, D.K. Ravishankar, S. Fattepur, G. Siddaraju, L. Nanjundaswamy, Validated electrochemical method for simultaneous resolution of tyrosine, uric acid, and ascorbic acid at polymer modified nano-composite paste electrode, Surf. Eng. Appl. Electrochem. 56 (2020) 415–426, https://doi.org/10.3103/S1068375520040134.
[40] D. Zhang, Y. Zhang, L. Zheng, Y. Zhan, L. He, Graphene oxide/poly-L-lysine assembled layer for adhesion and electrochemical impedance detection of leukemia K562 cancer cells, Biosens. Bioelectron. 42 (2013) 112–118, https://doi.org/10.1016/j.bios.2012.10.057.
[41] S. He, Z. Chen, Y. Yu, L. Shi, A novel non-enzymatic hydrogen peroxide sensor based on poly-melamine film modified with platinum nanoparticles, RSC Adv. 4 (2014) 45185–45190, https://doi.org/10.1039/C4RA06925K.
[42] F. Liu, M.H. Jang, H.D. Ha, J.H. Kim, Y.H. Cho, T.S. Seo, Facile synthetic method for pristine graphene quantum dots and graphene oxide quantum dots: Origin of blue and green luminescence, Adv. Mater. 25 (2013) 3657–3662, https://doi.org/10.1002/adma.201300233.
[43] S.N. Baker, G.A. Baker, Luminescent carbon nanodots: emergent nanolights, Angew. Chem. Int. Ed. 49 (2010) 6726–6744, https://doi.org/10.1002/anie.200906623.
[44] J.S.G. Selva, A. Sukeri, R.P. Bacil, S.H.P. Serrano, M. Bertotti, Electrocatalysis of the hydrogen oxidation reaction on a platinum-decorated nanoporous gold surface studied by scanning electrochemical microscopy, Electroanal. Chem. 934 (2023) 117302, https://doi.org/10.1016/j.jelechem.2023.117294.
[45] R. Kaimal, V. Vinoth, A.S. Salunke, H. Valdes, R.V. Mangalaraja, B. Aljafari, S. Anandan, Highly sensitive and selective detection of glutathione using ultrasonic aided synthesis of graphene quantum dots embedded over amine-functionalized silica nanoparticles, Ultrason. Sonoche. 82 (2022) 105868, https://doi.org/10.1016/j.ultsonch.2021.105868.
[46] V. Vinoth, L.N. Natarajan, R.V. Mangalaraja, H. Valdes, S. Anandan, Simultaneous electrochemical determination of dopamine and epinephrine using gold nanocrystals capped with graphene quantum dots in a silica network, Microchim Acta 186 (2019) 681, https://doi.org/10.1016/j.carbon.2012.06.002.
[47] Y. Dong, J. Shao, C. Chen, H. Li, R. Wang, Y. Chi, X. Lin, G. Chen, Blue luminescent graphene quantum dots and graphene oxide prepared by tuning the carbonization degree of citric acid, Carbon 50 (2012) 4738–4743, https://doi.org/10.1016/j.carbon.2012.06.002.
[48] C. Zhao, Z. Liu, W. Xu, M. Chen, S. Weng, L. Xu, Q. Cai, A glassy carbon electrode based on graphene quantum dots (GQDs) for simultaneous detection of acetaminophen and ascorbic acid, Anal. Methods 7 (2015) 8877–8881, https://doi.org/10.1039/C5AY02236C.
[49] M.I. Majeed, E.A.M. Al-Jawadi, Electrochemical biosensors for determination of anticancer medicine etoposide in human blood by glassy carbon modified electrode based on film of poly (L-lysine) with MWCNTS, J. Phys. Conference Series 1660 (2020) 012092, https://doi.org/10.1088/1742-6596/1660/1/012092.
[50] B. Rezaei, H. Khosropour, A.A. Ensafi, M. Dinari, A. Nabyian, A new electrochemical sensor for the simultaneous determination of guanine and adenine: using NiAl-layered double hydroxide/graphene oxide-multi wall carbon nanotubes modified glassy carbon electrode, RSC Adv. 5 (2015) 75756–75765, https://doi.org/10.1039/C5RA15845A.
[51] G. Wang, G. Shi, X. Chen, R. Yao, F. Chen, A glassy carbon electrode modified with graphene quantum dots and silver nanoparticles for simultaneous determination of guanine and adenine, Microchim. Acta 182 (2015) 315–322, https://doi.org/10.1007/s00604-014-1335-1.
[52] C. Raril, J.G. Manjunatha, A simple approach for the electrochemical determination of vanillin at ionic surfactant modified graphene paste electrode, Microchem. J. 154 (2020) 104575, https://doi.org/10.1016/j.microc.2019.104575.
[53] L. Zou, Y. Li, B. Ye, Voltammetric sensing of guanine and adenine using a glassy carbon electrode modified with a tetraoxocalix[2]arene[2]triazine Langmuir-Blodgett film, Microchim. Acta 173 (2011) 285–291, https://doi.org/10.1007/s00604-011-0563-x.